

The structure of allelic diversity in the presence of purifying selection.

Michael M. Desai¹, Aleksandra M. Walczak², and Joshua B. Plotkin³

*¹Department of Organismic and Evolutionary Biology,
Department of Physics, and
FAS Center for Systems Biology, Harvard University*

*²CNRS-Laboratoire de Physique Théorique de l'École Normale Supérieure,
24 rue Lhomond, 75005 Paris, France,*

³Department of Biology, University of Pennsylvania

(Dated: June 5, 2022)

Abstract

In the absence of selection, the structure of allelic diversity is described by the elegant sampling formula of Ewens. This formula has helped shape our expectations of empirical patterns of molecular variation. Along with coalescent theory, it provides statistical techniques for rejecting the null model of neutrality. However, we still do not fully understand the statistics of the allelic diversity we expect to see in the presence of natural selection. Earlier work has described the effects of strongly deleterious mutations linked to many neutral sites, and allelic variation in models where offspring fitness is unrelated to parental fitness, but it has proven difficult to understand allelic diversity in the presence of purifying selection at many linked sites. Here, we study the population genetics of infinitely many perfectly linked sites, some neutral and some deleterious. Our approach is based on studying the lineage structure within each class of individuals of similar fitness in the deleterious mutation-selection balance. Analogous to the Ewens sampling formula, we derive expressions for the likelihoods of any configuration of allelic types in a sample. We find that for moderate and weak selection pressures the patterns of allelic diversity cannot be described by a neutral model for any choice of the effective population size, indicating that there is power to detect selection from patterns of sampled allelic diversity.

Running Head: Allelic Diversity and Purifying Selection

Keywords: Allelic Diversity, Purifying Selection, Ewens Sampling Formula, Linkage

Corresponding Author:

Joshua B. Plotkin

Department of Biology

University of Pennsylvania

219 Lynch Labs

433 S. University Avenue

Philadelphia, PA 19104

215-573-8052

jplotkin@sas.upenn.edu

INTRODUCTION

Natural selection distorts patterns of genetic variation from their neutral expectation. Recent evidence suggests that such distortions may be quite common, which has led to increasing interest in understanding precisely how selection alters patterns of molecular evolution (HAHN, 2008). Theoretical developments have produced a good understanding of how positive selection at a few sites affects genetic variation at linked neutral sites (BARTON, 1998; BARTON and ETHERIDGE, 2004; GILLESPIE, 2001, 2000) and of how strong purifying selection at many sites affects variation at linked neutral sites (CHARLESWORTH, 1994; CHARLESWORTH *et al.*, 1993, 1995). An alternative approach developed by SAWYER and HARTL (1992) and HARTL and SAWYER (1994) has explored variation at the selected sites themselves, but only when these sites are freely recombining (BUSTAMANTE *et al.*, 2001).

These existing bodies of work describing the effects of selection have been used as a basis for interpreting patterns of genetic variation observed in natural populations. But an important gap still remains: we do not understand the patterns of genetic variation we expect to see when weak or moderate selection acts on many linked selected sites. Such selection pressures are often referred to as Hill-Robertson interference (HILL and ROBERTSON, 1966), and simulations have shown they can have a significant impact on sequence variation (COMERON and KREITMAN, 2002; MCVEAN and CHARLESWORTH, 2000; SEGER *et al.*, 2010). Moreover, recent sequence data from a variety of populations indicates that the types of deviations caused by Hill-Robertson interference may be common in nature (BETANCOURT *et al.*, 2009; COMERON and KREITMAN, 2002; COMERON *et al.*, 2008; HAHN, 2008; SEGER *et al.*, 2010).

In this paper, we analyze the expected patterns of allelic diversity in the presence of purifying selection at many perfectly linked sites. We study the diversity generated by mutations both at the negatively selected sites themselves and at linked neutral sites, in an infinite-sites/infinite-alleles framework. Our analysis produces a version of the neutral Ewens sampling formula that is valid in the presence of negative selection. Our approach is valid for both weak and strong selection.

Over the past few decades, numerous authors have studied diversity in infinite-alleles frameworks that incorporate selection. LI (1977) and WATTERSON (1978) introduced models

in which alleles may have a few different selective effects. These models have been studied by various other authors (EWENS and LI, 1980; GRIFFITHS, 1983; LI, 1978, 1979). More recent work has analyzed a very general model of selection introduced by ETHIER and KURTZ (1987), which allows for diverse types of selection pressures (ETHIER and KURTZ, 1994; GROTE and SPEED, 2002; JOYCE, 1995; JOYCE and TAVARE, 1995). This work has helped us understand the general effects of selection in distorting the frequency spectrum of sampled alleles. However, the models these authors have analyzed do not have any natural correspondence to a concrete picture of mutations and selection occurring at specific sites. Rather, they assume that each new mutation creates a new allele whose fitness is completely independent of the fitness of its parent. In other words, there is no sense of relatedness among alleles, or of a correlation in fitness between closely related alleles.

In this paper we take a different approach, based on a specific model of linked sites. We imagine that each individual has a genome comprised of many neutral and many negatively selected sites. The fitness of each individual is determined by the number of mutations it carries at the negatively selected sites. We make the infinite-sites assumption that no two mutations at the same site ever segregate simultaneously. This is also an infinite-alleles model, but it is based on a specific model of mutations at individual sites, and the fitness of each new allele depends on the fitness of its parent. The balance between mutations at deleterious sites and selection against them leads to a steady state mutation-selection balance (HAIGH, 1978). Our approach is to study the structure of lineages within this steady state.

CHARLESWORTH *et al.* (1993) proposed an approximation known as background selection (BGS) to characterize genetic diversity in the same model we analyze here. The BGS approach is based on the idea that individuals who acquire deleterious mutations are purged quickly from the population, so that all such individuals are recently descended from mutation-free individuals. Hence the genetic diversity is characteristic of a neutral population at a reduced effective population size (CHARLESWORTH, 1994; CHARLESWORTH *et al.*, 1995). Our approach is in some respects a generalization of background selection to accommodate weaker selection pressures. In particular, our analysis of genetic variation applies even when deleterious mutants survive for a substantial period of time before being eliminated by selection. Most importantly, we find that in this regime the expected patterns of genetic diversity cannot be described by neutral theory with some appropriately chosen

effective population size. This result is fundamentally different than background selection, and it means that we can hope to unambiguously detect the action of negative selection, distinct from neutrality with a lower effective population size.

Our analysis in this paper is limited to allelic diversity, and it does not address the relationship among sampled alleles. In other words, our analysis only tells us the probability that individuals are genetically identical, not the distribution of the number of specific sites at which individuals may differ. Our results are thus not directly comparable to background selection, which makes predictions about expected diversity at the level of individual sites. However, while our allele-based results provide an incomplete picture of genetic diversity within the population, they do provide a useful perspective on how purifying selection distorts patterns of molecular evolution. We would of course like to extend our analysis to predict the expected patterns of variation at the level of individual sites. In DESAI *et al.* (2010) we use the framework laid out in this paper as the basis for understanding this more general problem. However, in this paper we focus exclusively on the more limited analysis of allelic diversity, which provides an essential background for the analysis of the more general problem in DESAI *et al.* (2010).

We begin by describing the details of our model. We then describe the form of the steady state deleterious mutation-selection balance, and use this to calculate the structure of allelic diversity within the population. Finally, we use these results to calculate various statistics describing the allelic diversity in a sample of individuals from the population, and we compare these results to monte carlo simulations and to neutral theory.

MODEL

We imagine a finite haploid population of constant size N . Each haploid genome has a large number of sites, which begin in some ancestral state and mutate at some constant rate. Each mutation is either neutral or confers some fitness disadvantage s (where by convention $s > 0$). We assume an infinite-sites framework, so there is negligible probability that two mutations segregate simultaneously at the same site.

We assume that there is no epistasis for fitness, and that each deleterious mutation carries fitness cost s , so that the fitness of an individual with k deleterious mutations is $w_k = (1-s)^k$. Since we assume that $s \ll 1$, we will often approximate $w_k = 1 - sk$. Later we comment

briefly on extensions to our method to consider the case when the selection coefficient of a deleterious mutations is drawn from some fixed distribution.

The population dynamics are assumed to follow the diffusion limit of the standard Wright-Fisher model. That is, in each generation each new individual acquires a deleterious mutation somewhere in its genome with probability U_d . We define $\theta_d/2 \equiv NU_d$, the per-genome scaled deleterious mutation rate. Similarly, neutral mutations occur at a rate U_n per individual per generation, and we analogously define $\theta_n/2 \equiv NU_n$. We assume that each newly arising mutation occurs at a site at which there are no other segregating polymorphisms in the population (the infinite-sites assumption). Since in this paper we focus only on allelic diversity, this infinite-sites approximation simply means that each new mutation creates a unique allele. Throughout the analysis we assume that Muller's ratchet can be neglected; we discuss the validity of this approximation in the Discussion.

We study the case of perfect linkage. In other words, we imagine that all the sites we are considering are in an asexual genome or within a short enough distance in a sexual genome that recombination can be entirely neglected. Although our model is defined for haploids, this assumption means that our analysis also applies to diploid populations provided that there is no dominance (i.e. being homozygous for the deleterious mutation carries twice the fitness cost as being heterozygous).

We believe that this is the simplest possible model based on a concrete picture of mutations at individual sites that can describe the effects of a large number of linked negatively selected sites on patterns of genetic variation.

ANALYSIS

The balance between mutations and selection leads to a steady state distribution of fitness within the population; this is the well-known mutation-selection balance. However, each class of individuals with the same fitness is not genetically homogeneous, but rather contains a number of different alleles. The number and frequency distribution of these alleles depends on how quickly new alleles are created by deleterious mutations from more-fit individuals, and hence on the overall fitness distribution. Conversely, the total frequency of all individuals at a given fitness must equal the sum of all the frequencies of alleles in that fitness class. This requirement for self-consistency between the steady state distribution of fitness within

the population and the genetic diversity within each class of individuals at a given fitness is the basic idea behind our analysis. We begin by describing the relevant aspects of the mutation-selection balance that leads to a steady state distribution of fitness within the population.

The steady state fitness distribution:

In our model, all deleterious mutations have the same fitness cost s , so we can characterize individuals by their Hamming class, k , relative to the wildtype (which by definition has $k = 0$). That is, individuals in class k have k deleterious mutations more than the most-fit individuals in the population. Here k refers only to the number of *deleterious* mutations an individual has; individuals with the same k can have different numbers of neutral mutations. We normalize fitness such that by definition all individuals in class $k = 0$ have fitness 1. Individuals in class k then have fitness $1 - ks$.

Imagine that at a given time a fraction $h_k(t)$ of the population is in class k . This class is acquiring new individuals due to deleterious mutations arising in class $k - 1$, and it is losing individuals due to deleterious mutations away to class $k + 1$. It also gains or loses individuals at a rate $-(k - \bar{k})s$ due to selection, where \bar{k} is the mean k within the population, $\bar{k} \equiv \sum k h_k$. This is illustrated in Fig. 1. Note that the term involving \bar{k} simply normalizes the effect of selection (selection favors a class if it is more fit than the average individual, and vice versa). This means that on average $h_k(t)$ will evolve according to the equation

$$\frac{dh_k(t)}{dt} = U_d h_{k-1} - U_d h_k - (k - \bar{k}) h_k s. \tag{1}$$

Note this is a system of k equations for all the $h_k(t)$. Of course random genetic drift will also affect the $h_k(t)$, and these deterministic equations are only true on average. We return to this point below, but for now we neglect drift and focus on the steady state distribution.

The steady state fitness distribution (the mutation-selection balance) is given by the values of $h_k(t)$ after a long time. We can find this mutation-selection balance by setting the right hand side of Eq. (1) equal to 0 for all values of k . This calculation was originally carried out by HAIGH (1978); he found that the steady state, \hat{h}_k , is given by a Poisson distribution with mean $\frac{U_d}{s}$,

$$\hat{h}_k = e^{-U_d/s} \frac{U_d^k}{k! s^k}. \tag{2}$$

Note that this means that the average fitness in the population is $1 - U_d$, and that $\bar{k} = \frac{U_d}{s}$.

Allelic diversity within a given fitness class:

We now shift to the other half of our self-consistent approach, and look more closely at individuals within a given fitness class, as illustrated in Fig. 1b. For the moment we neglect neutral mutations; we consider their effects further below.

All lineages in class k originally arose from a mutation to an individual that was in class $k - 1$. Each new deleterious mutation from an individual in class $k - 1$ founds a new lineage within class k . Such lineages are founded at a rate $\theta_k/2$, where we define

$$\theta_k = 2Nh_{k-1}U_d. \quad (3)$$

Note this is true whether or not the h_k are at their steady-state values, though for the purposes of our analysis we will always assume the steady state.

In our infinite-alleles approximation, each new lineage is an allele that is unique within the population. The fate of this lineage (allele) is then determined by the forces of random drift, selection, and additional mutations. Additional mutations that occur within this lineage go on to found new alleles. Thus from the point of view of this particular lineage, additional mutations cause individuals to be lost from the lineage. This means that individuals are removed from a lineage in class k at a per capita rate

$$s_k \equiv -U_d - s(k - \bar{k}). \quad (4)$$

We refer to s_k as the *effective selection coefficient* against an allele in class k , because it is the rate at which any particular lineage in class k loses individuals. Note that s_k depends implicitly on the h_k through the term involving \bar{k} (recall \bar{k} is the average value of k , $\bar{k} \equiv \sum kh_k$). For convenience we will define the scaled effective selection coefficient γ_k by

$$\gamma_k = Ns_k. \quad (5)$$

Note that in steady state, when the fitness distribution h_k takes the mutation-selection balance form \hat{h}_k derived above, $\bar{k} = U_d/s$ and the effective selection coefficient s_k is negative for all fitness classes with $k > 0$. This makes intuitive sense: each fitness class (except $k = 0$) is constantly receiving new individuals due to mutations. Thus older individuals must on average die out, if the fitness class is to stay at a constant steady state size. The only exception is the $k = 0$ class, for which $s_k = 0$. This class drifts effectively neutrally, with its

actual selective advantage relative to the mean exactly balanced by the loss of individuals due to deleterious mutations. For $k = 1$ we have $s_1 = -s$, and in general $s_k = -ks$. On the other hand, θ_k/h_k increases with k , reflecting the fact that the stronger selection against the larger- k classes is balanced by a larger influx of new deleterious mutations into these classes.

We can now incorporate the effect of neutral mutations. Each neutral mutation within an individual in class k creates a new lineage in class k . Thus we may simply redefine the rate at which new lineages are founded, giving

$$\theta_k \equiv 2Nh_{k-1}U_d + 2Nh_kU_n. \quad (6)$$

Each neutral mutation also causes an individual to be lost from the lineage it was in before the mutation, so we also redefine the effective selection coefficient

$$s_k \equiv -U_d - U_n + s(k - \bar{k}). \quad (7)$$

These neutral mutations are also reflected in Fig. 1b. Note that for all k , neutral mutations tend to increase θ_k , and make s_k more negative. In the presence of neutral mutations, even s_0 is negative.

We have seen that new lineages are founded within fitness class k at rate $\theta_k/2$, and then drift randomly subject to an effective selective pressure s_k . We now make the key assumption that each lineage is independent of all the others. This assumption is valid provided that no lineage ever becomes a substantial fraction of the overall population, which will be true whenever $N|s_k| \gg 1$ (i.e. all lineages are selected against strongly enough). A sufficient condition for this to hold is simply $N(U_n + U_d) \gg 1$, and in fact our approximation will also hold even in some circumstances when this condition breaks down (we describe this further below).

Using the independence assumption, we have reduced the problem of describing a lineage within a given fitness class to exactly the situation addressed by the Poisson Random Field model of SAWYER and HARTL (1992). Thus the frequency distribution of lineages (alleles) in fitness class k is a Poisson Random Field (PRF) with parameters θ_k and γ_k (where as before $\gamma_k \equiv Ns_k$). That is, the number of distinct lineages in class k segregating at a frequency between a and b in the entire population is Poisson distributed with mean

$$\int_a^b f_k(x) dx, \quad (8)$$

where

$$f_k(x) = \frac{\theta_k}{x(1-x)} \frac{1 - e^{-2\gamma_k(1-x)}}{1 - e^{-2\gamma_k}}. \quad (9)$$

This is equivalent to saying that the probability that there exists a lineage in class k with frequency between x and $x + dx$ is $f_k(x)dx$, for infinitesimal dx . Note that this PRF result implicitly assumes that θ_k and γ_k are constant (which requires constant h_k), and hence only describes the diversity in steady state.

The self-consistency condition:

It is clear from our PRF formulation above that the allelic diversity within each fitness class depends on the θ_k and γ_k , which in turn depend on the h_k . Yet the sum of the frequencies of all the alleles within fitness class k is, by definition, h_k . In steady state, these two quantities must be equal. More specifically, since we have derived the steady state value of h_k in Eq. (2),

$$h_k = e^{-U/|s|} \frac{(U/|s|)^k}{k!},$$

when we plug these h_k into our PRF result, the summed allele frequencies according to the PRF must agree with steady-state value we used for h_k , for consistency.

According to our PRF result, the sum of the frequencies of all the alleles in fitness class k is

$$h_k = \int_0^1 x f_k(x) dx. \quad (10)$$

Consistency thus requires that

$$e^{-U/|s|} \frac{(U/|s|)^k}{k!} = \int_0^1 x f_k(x) dx = \int_0^1 x \cdot \frac{\theta_k}{x(1-x)} \frac{1 - e^{-2\gamma_k(1-x)}}{1 - e^{-2\gamma_k}} dx, \quad (11)$$

where θ_k and γ_k depend on N, U_d, U_n, s and the h_k as defined above. Because Eq. (2) is equivalent to requiring $\theta_k/2 = |\gamma_k|h_k$ for all k , we can rewrite the self-consistency equation as

$$\frac{\theta_k}{2|\gamma_k|} = \int_0^1 x \cdot \frac{\theta_k}{x(1-x)} \frac{1 - e^{-2\gamma_k(1-x)}}{1 - e^{-2\gamma_k}} dx. \quad (12)$$

Some algebra reduces this to the condition

$$\int_0^1 \frac{1 - e^{-2\gamma_k x}}{x} dx = \frac{1 - e^{-2\gamma_k}}{2|\gamma_k|}. \quad (13)$$

The analysis in Appendix A shows that this condition holds whenever $|\gamma_k| \gg 1$. When this is true, the steady state mutation-selection balance of Eq. (2) is also the distribution h_k that makes our PRF analysis of the allelic diversity within each fitness class self-consistent.

The condition $|\gamma_k| \gg 1$ corresponds to saying that the effective selection coefficient in each class is large compared to $1/N$. This will be true for all k whenever $NU_n \gg 1$. Here U_n is the total mutation rate to neutral mutations within the linked region of the genome we are considering. And in practice, even a slightly weaker condition is sufficient, because even when it fails in some fitness classes our analysis is still valid for all classes in which $|\gamma_k| \gg 1$. Thus even if the most-fit low- k classes do not satisfy this condition, our results still give a good approximation to the population allelic diversity provided $|\gamma_k| \gg 1$ for the classes around \bar{k} that make up the bulk of the population. This will hold whenever $\gamma_{\bar{k}} = N(U_d + U_n) \gg 1$. Thus whenever *either* $NU_d \gg 1$ or $NU_n \gg 1$, the consistency equation holds and our analysis provides a good description of the allelic diversity within the population.

Our analysis leading to the steady state mutation-selection balance, Eq. (2), is valid even when $N(U_d + U_n) < 1$. Thus the fact that this fitness distribution h_k does not lead to a self-consistent result in this parameter regime must be because our PRF result for the allelic diversity within each fitness class is inaccurate. And indeed, as noted above, this PRF result relies on the assumption that all mutant lineages segregate independently, which requires $|\gamma_k| \gg 1$. When this fails, the growth of some mutant lineages is limited by the size of the population, which is ignored by the PRF approximation. Thus the PRF approximation overestimates the probability that lineages become common (i.e. for large x , $f_k(x)$ is too big). This means that our approximation will predict $\int x f_k(x)$ is too large, and hence the self-consistency breaks down.

Sampling Formulas:

We can now use our results for the distribution of allelic diversity within each fitness class to calculate the probability of sampled configurations of allelic types. Our goal is to calculate the probability that a sample of n individuals will have some distribution of allelic types (e.g. n_1 individuals with allele 1, n_2 individuals with allele 2, etc.). Specifically, we aim to calculate a negative selection version of the neutral Ewens sampling formula (ESF).

We begin with the simplest case, a sample of $n = 2$ individuals from the population. What is the chance that these individuals are the same genotype? In other words, what is the allelic homozygosity in the population? In order to be the same genotype, the two individuals must carry the same number of deleterious mutations — i.e. they must fall in the

same Hamming class, k . In addition, they must also be of the same mutant lineage within class k . This latter probability is equal to the expected value of x^2 , where x is integrated over the distribution of lineage frequencies in class k . Thus, the full probability that two sampled individuals have the same genotype, which we denote Q_2 , is given by

$$Q_2 = \sum_{k=0}^{\infty} \int_0^1 x^2 f_k(x) dx, \quad (14)$$

where $f_k(x)$ is given by Eq. (9) in terms of the mutation rates U_d and U_n , the population size N , and the selective effect of each mutation s . We evaluate this integral in Appendix A; we find

$$Q_2 = \sum_{k=0}^{\infty} \frac{h_k}{2Ns_k}. \quad (15)$$

To our knowledge, this expression is the first theoretical prediction for the steady state homozygosity involving many linked selected sites.

Similarly, the chance that two sampled individuals will be different allelic types (i.e. the heterozygosity) is given by $Q_{1,1}$:

$$Q_{1,1} = \sum_k \int_0^1 x(1-x) f_k(x) dx. \quad (16)$$

Note that

$$Q_{1,1} = \sum_k \int_0^1 x f_k(x) dx - \sum_k \int_0^1 x^2 f_k(x) dx \quad (17)$$

$$= \sum_k h_k - Q_2 \quad (18)$$

$$= 1 - Q_2, \quad (19)$$

where the last two equalities follow from our consistency condition, Eq. (11). In other words, to the accuracy with which our basic self-consistency condition holds, our expressions for $Q_{1,1}$ and Q_2 sum to one, as they should.

Let us consider the probabilities of possible configurations in a sample of size $n = 3$, namely Q_3 , $Q_{2,1}$, and $Q_{1,1,1}$. Similar to the calculation above,

$$Q_3 = \sum_k \int x^3 f_k(x) dx. \quad (20)$$

The probability the sample will take a $\{2, 1\}$ allelic configuration is slightly more tricky. This can arise only if two of the sampled alleles are the same type, provided the third is not of that type, i.e.

$$Q_{2,1} = \sum_k \int 3x^2(1-x)f_k(x) dx. \quad (21)$$

The factor 3 arises because there are $\binom{3}{2}$ possible pairs of identical individuals in a sample of size 3. We can define $Q_{1,1,1}$ as $1 - Q_{2,1} - Q_3$.

Another way to calculate $Q_{2,1}$, which we will utilize in more complicated calculations below, is to let x denote the frequency in the population of the allele that is sampled twice and let y denote the frequency in the population of the allele that is sampled once, and introduce the notation

$$Q_{2,1} \sim 3x^2y - 3x^3 \quad (22)$$

by which we mean that we should integrate over both variables for any terms involving products. That is,

$$Q_{2,1} = \sum_k \int_0^1 \sum_l \int_0^1 3x^2y f_k(x) f_l(y) dy dx - \sum_k \int_0^1 3x^3 f_k(x) dx \quad (23)$$

$$= 3 \left(\sum_l \int_0^1 y f_l(y) dy \right) \left(\sum_k \int_0^1 3x^2 f_k(x) dx \right) - \sum_k \int_0^1 x^3 f_k(x) dx \quad (24)$$

$$= 3 \cdot 1 \cdot \sum_l \int_0^1 x^2 f_k(x) dx - \sum_l \int_0^1 3x^3 f_k(x) dx \quad (25)$$

$$= \sum_k \int 3x^2(1-x)f_k(x) dx, \quad (26)$$

which agrees with our earlier expression for $Q_{2,1}$.

As we did for Q_2 , we can evaluate the integrals in the Q_3 and $Q_{2,1}$ expressions explicitly using the calculations described in Appendix A. We find

$$Q_3 = \sum_k \frac{h_k}{2(Ns_k)^2}, \quad (27)$$

$$Q_{2,1} = 3 \sum_k \frac{h_k}{2Ns_k} \left(1 - \frac{1}{Ns_k} \right). \quad (28)$$

Note that these results depend on powers of N in a similar way to the neutral ESF, while the dependence on s_k is of the same form as the dependence on U_n in the neutral ESF.

Using the notation introduced above, we can list the probabilities of all configurations among $n = 4$ samples:

$$Q_4 \sim x^4 \tag{29}$$

$$Q_{3,1} \sim 4x^3(1-x) \tag{30}$$

$$Q_{2,2} \sim 3x^2y^2 - 3x^4 \tag{31}$$

$$Q_{2,1,1} \sim 6x^2 - 12x^3 + 12x^4 - 6x^2y^2 \tag{32}$$

$$Q_{1,1,1,1} = 1 - Q_4 - Q_{3,1} - Q_{2,2} - Q_{2,1,1}. \tag{33}$$

In an analogous way, we can in principle write down the probabilities of all possible configurations of allelic types in a sample of any size n . This provides an analytic prescription for finding the probability of any possible configuration of allelic types among n sampled individuals. Taken together, these expressions are a sampling formula analogous to Ewens' result in the neutral case, which could in principle be used to make inferences from data about population sizes, mutation rates, and selection pressures. In practice, these expressions become increasingly unwieldy for large n . Further, for applications to inference from modern data, we will generally want a method that looks at per-site diversity rather than allelic diversity, which we develop in DESAI *et al.* (2010). Thus we do not pursue the large- n sampling formulae further here. Instead, we focus on small samples, using these to illustrate the essential ways in which linked deleterious mutations alter allelic diversity.

In order to calculate the probability of any particular allelic configuration, we must perform the relevant sums and integrals in the corresponding sampling formula. All such integrals involve combinations of polynomial functions multiplied by exponentials, and they can be integrated exactly in terms of elementary functions and (in a few cases) the exponential integral function $Ei(a) \equiv \int_0^1 \frac{e^{ax}}{x}$. The exponential integral function can then be approximated accurately in terms of elementary functions in the $N(U_n + U_d) \gg 1$ regime we are considering, as we discuss in Appendix A. While we make use of analytical evaluations of the sums over k in certain regimes in a few places below to make general conceptual points, in practice it is easier to simply numerically evaluate the sums involved in each sampling formula. Because the sums are all well-behaved, such numerical calculations are very fast and accurate.

A distribution of fitness effects of deleterious mutations:

We have analyzed a model in which all deleterious mutations have the same fitness cost, s . However, in most real populations it is likely that deleterious mutations have a range of possible fitness effects. We could model this by assuming that the overall deleterious mutation rate is still U_d , but that deleterious mutations have a fitness cost between s and $s + ds$ with probability $\rho(s)ds$. That is, $\rho(s)$ is the distribution of fitness effects of deleterious mutations.

In this more general situation, there is still a steady state distribution of fitness within the population. Generalizing our earlier notation, we can write this distribution as $h(k)$, where $Nh(k)$ is the steady state number of individuals with a fitness between sk and $(s + ds)k$, where s is the average fitness cost of a deleterious mutation and k is no longer constrained to be an integer. For certain $\rho(s)$ (e.g. an exponential distribution) it is possible to calculate $h(k)$ analytically, but even when this is not possible there does exist some steady state $h(k)$.

The basic ideas behind our analysis still apply in this more general situation. The rate at which new lineages within fitness “class” $h(k)$ are created is now

$$\theta(k)/2 = Nh(k)U_n + N \int_0^k h(k')\rho((k - k')/s)dk'. \quad (34)$$

The effective selection pressure against individuals in this class is

$$s(k) = U_n + U_d - (k - \bar{k})s. \quad (35)$$

Using these modified parameters, we can now apply our analysis as before; the distribution of lineage frequencies in class k is given by the PRF formula $f(k; x)$ with appropriate $\theta(k)$ and $s(k)$. We can then find sampling formulas as before — the only difference is that instead of summing over a discrete set of fitness classes, we must integrate over a continuous set of possible fitnesses. For example, we have $Q_2 = \int_0^\infty \int_0^1 x^2 f(k, x) dx dk$.

This extension of our model allows us to calculate the effects of more general forms of purifying selection on allelic diversity. However, there are a wide array of possible distributions $\rho(s)$, and using this more general form obscures the basic effects of selection. Thus in analyzing our results and comparing to simulations we focus on the simpler case in which all deleterious mutations have the same fitness cost s . This focus has the advantage of simplicity, and it allows us to explore more clearly how the strength of selection affects the patterns of allelic diversity.

Simulations:

In order to check the validity of our analysis, we have performed Monte-Carlo simulations of a Wright-Fisher population. In our simulations, we consider a population of constant size N and we keep track of the frequencies of all genotypes over successive, discrete generations. In each generation, N individuals are sampled with replacement from the preceding generation, according to the standard Wright-Fisher multinomial sampling procedure (EWENS, 2004) in which the chance of sampling an individual is determined by its fitness relative to the population mean fitness.

In our simulations, each genotype is characterized by the set of sites at which it harbors deleterious mutations and the set of sites at which it harbors neutral mutations. In each generation, a Poisson number of deleterious mutations are introduced, with mean NU_d , and a Poisson number of neutral mutations are introduced, with mean NU_n ; each new mutation is ascribed to a novel site, indexed by a random number. The mutations are distributed randomly and independently among the individuals in the population (so that a single individual might receive multiple mutations in a given generation).

Starting from a monomorphic population, all simulations were run for at least $\frac{1}{s} \ln(U_d/s)$ generations, to ensure relaxation both to the steady-state mutation-selection equilibrium and to the PRF equilibrium of allelic frequencies within each fitness class. The final state of the population – i.e. the frequencies of all surviving genotypes – was recorded at the last generation. In most of the parameter regimes we explored, Muller’s ratchet proceeded during the simulation, so that the least loaded class at the end of each simulation typically contained at least 10 deleterious mutations, and often many more.

For each set of a parameter values, (N, U_n, U_d, s) , we ran at least 50 replicate simulations with different pseudo-random seeds. From the final population we sampled at least 20,000 pairs or triplets of individuals, and we compared their genotypes to estimate the values of Q_2 , $Q_{2,1}$, and $Q_{1,1,1}$ in each replicate. We then averaged these values across the replicates to produce the points shown in Figure 2.

RESULTS AND DISCUSSION

Using the approach we have described, we can calculate the probability of any allelic configuration within a sample of n individuals from a population experiencing negative selection

at many linked sites. From this, we can calculate the expected distribution of any statistic describing allelic diversity. To do so we must first determine which allelic configurations lead to what values of the statistic. The probability of each possible value of the statistic is then the sum of the probabilities of all allelic configurations leading to that value. This is identical to the calculation we would do in the neutral case — the only difference is that to calculate the probability of each allelic configuration, we use our sampling formula rather than the neutral Ewens sampling formula.

In practice, some statistics are easier to calculate than others, because for large n our sampling formulas become very complex. While we can easily calculate the distribution of statistics describing diversity in a small sample, further work is needed to develop efficient methods of calculating certain important statistics in large samples (e.g. the number of segregating alleles in a sample of size n , K_n , for large n). This is clearly important for applications of our method to analysis of sequence data, but the combinatoric and computational issues involved are an extensive topic which is tangential to the ideas underlying our method. Instead, we focus here on describing the distributions of simple statistics involving small samples. Our aim is to highlight the essential differences between neutral diversity and the diversity in situations involving linked deleterious mutations.

Relationship to the neutral Ewens sampling formula:

Although it may seem counterintuitive, our analysis applies even when $U_d = 0$ (that is, in the case where all mutations are neutral). In this case, all genotypes are in the fitness class $k = 0$, and we have $\gamma_0 = -NU_n$ and $\theta_0 = \theta = 2NU_n$. Provided that $|\gamma_0| \gg 1$, the conditions for our PRF analysis to be valid are met, and all of our previous results still apply, but are greatly simplified.

In this neutral case, our model is the same as that studied by (EWENS, 1972), and hence we expect our results should reduce to the neutral Ewens sampling formula. We can see that this is indeed true in the case of $n = 2$ sampled individuals, where our expression for the expected homozygosity in the neutral case is

$$Q_2 = \frac{h_0}{2Ns_0} = \frac{1}{2NU_n} = \frac{1}{\theta}, \tag{36}$$

which is equal to the Ewens sampling formula (ESF) result

$$Q_2^{ESF} = \frac{1}{1 + \theta} \tag{37}$$

in the large- θ limit where our analysis applies. Similarly our result for the probability $Q_{2,1}$,

$$Q_{2,1} = 3 \left[\frac{h_0}{2Ns_0} - \frac{h_0}{Ns_0} \right] = \frac{3}{\theta} - \frac{2}{\theta^2} \quad (38)$$

is equivalent to the neutral Ewens sampling formula result

$$Q_{2,1}^{ESF} = \frac{3\theta}{(1+\theta)(2+\theta)}, \quad (39)$$

in the large- θ limit. Analogous calculations, using the results from Appendix A, show that the probabilities of allelic configurations in larger samples are similarly identical to the neutral Ewens sampling formula to first order in $1/\theta$ (i.e. in the $\theta \gg 1$ limit).

For nonzero U_d , we expect that our results will differ from the predictions of the neutral ESF. To illustrate these differences in more detail, we study the allelic configurations in samples of size $n = 2$ and $n = 3$. Consider first the homozygosity Q_2 in a sample of size $n = 2$. In Fig. 2a and c we show how Q_2 depends on U_d and the population size N for $U_n = 0$, both under our theory and in monte carlo simulations. We compare these results with the predictions of the neutral ESF. We make the same comparisons for the heterozygosity $Q_{2,1}$ in Fig. 2b and d. Analogous comparisons for nonzero U_n are shown in Fig. 3. We note that the simulation results agree well with our predictions and differ from those of the ESF.

In making this comparison, there is some ambiguity about how to interpret the ESF, which depends only on θ , for $U_d > 0$. In one interpretation, we neglect selection against the deleterious mutations and set $\theta = 2N(U_n + U_d)$; we refer to this as the NS-ESF case. Alternatively, we could neglect the deleterious mutations entirely and set $\theta = 2NU_n$; we refer to this as the NM-ESF case.

In Fig. 4 we explore the ambiguity in the interpretation of the ESF, and compare the predictions of our theory to the two different interpretations of the ESF. For small U_d , our prediction is equivalent to both interpretations of the neutral ESF. As U_d increases, our predicted homozygosity decreases slowly until it experiences a sharp transition at $U_d \approx s$. This transition makes intuitive sense: when $U_d < s$, most individuals in the population have no deleterious mutations, and hence the allelic diversity is similar to the NM-ESF. As U_d increases past s , most individuals have deleterious mutations, so these mutations decrease the expected homozygosity. These deleterious mutations decrease homozygosity by less than they would if they were neutral, so our predicted homozygosity is higher than the NS-ESF but lower than the NM-ESF.

We can gain further insight into this behavior by comparing our predictions to those of the NS-ESF and the NM-ESF. We see that even when $U_d = U_n$, our predicted homozygosity is only slightly lower than when $U_d = 0$, despite the fact that there are twice as many mutations occurring (and hence the NS-ESF prediction for Q_2 has declined by a factor of two). Here the NM-ESF prediction is fairly accurate, reflecting the fact that selection is still strong (with $U_d \ll s$) so that most individuals have no deleterious mutations at all. However, as U_d increases past s , most individuals now have one or more deleterious mutations and hence these mutations decrease our prediction for the allelic homozygosity. In this regime, the NM-ESF becomes inaccurate, because the deleterious mutations are sufficiently weakly selected ($U_d \gtrsim s$) that their presence is important to the diversity. However, despite this being weak selection, the fact that selection eliminates deleterious mutations from the population more rapidly than if they were neutral means that the allelic homozygosity is higher than the NS-ESF, even as U_d becomes very large. As U_d increases, our predictions become more similar to the NS-ESF, but even for very large U_d , our predictions differ from the NS-ESF by a factor of roughly 2 for these parameters. In Fig. 4b we show the “bizygosity” $Q_{2,1}$ as a function of U_d . Through this parameter range Q_3 is negligible, and so $Q_{1,1,1} \approx 1 - Q_{2,1}$. As Fig. 3b shows, the dependence of bizygosity on U_d is similar to the behavior of heterozygosity, for essentially the same reasons.

Our analysis above makes it clear that the difference between weak and strong selection is set by whether s is small or large compared to U_d . For $s \lesssim U_d$, selection is weak and the diversity generated by the deleterious mutations themselves can be important, and hence the NM-ESF is inaccurate. However provided that $Ns > 1$, selection is not so weak that the NS-ESF is accurate either; the selection against the deleterious mutations does reduce the amount of diversity they contribute. In this regime, neither interpretation of the Ewens neutral sampling formula provides an accurate prediction for allelic diversity. On the other hand, for $s \gg U_d$, selection is strong enough that the deleterious mutations are eliminated quickly from the population and hence do not contribute to diversity, and the NM-ESF is accurate. The NS-ESF is also accurate in this regime when $U_d \ll U_n$ but it will underestimate homozygosity when $U_d \gtrsim U_n$. Note that in Fig. 4 we show a case where $s > U_n$, so there is a regime where $s \gg U_d$ but $U_d \gtrsim U_n$ and hence the NM-ESF is accurate but the NS-ESF is not. Such a regime does not exist in the case $s < U_n$, but otherwise the

same qualitative patterns exist for the same reasons.

We explore the dependence on the strength of selection s further in Fig. 5, which shows our predictions for Q_2 and $Q_{2,1}$ as a function of s . The figure also compares our results to both the NM and the NS interpretations of the neutral Ewens sampling formula. We see that, consistent with the above discussion, for strong selection with $s \gg U_d$, the NM-ESF agrees with our predictions, as expected since deleterious mutations are quickly eliminated. When $s \lesssim U_d$, selection is weak and hence our predicted homozygosity (or $Q_{2,1}$) is smaller than the NM-ESF, but still larger than the NS-ESF (with the difference declining as s becomes of order U_n and becoming negligible when s gets so small that Ns becomes of order 1).

Comparison to the background selection approximation:

CHARLESWORTH *et al.* (1993) also studied the model we have considered, and developed an approximation to describe genetic diversity in the presence of many linked negatively selected sites. This approximation is widely used and has become known as background selection (BGS) (CHARLESWORTH, 1994; CHARLESWORTH *et al.*, 1995). The BGS analysis makes predictions about the genetic diversity at the level of individual sites, not just the allelic diversity we consider here. Further, it focuses on the genetic diversity among neutral mutations only. Thus it is not directly comparable to our results in this paper. Despite this, we find it instructive to briefly examine how BGS compares to our results, if we apply it to predict allelic diversity. We stress that this is not the interpretation intended by CHARLESWORTH *et al.* (1993) and does not provide a fair picture of its accuracy in general. Since BGS describes the structure of genealogies, we defer a detailed discussion of the accuracy of the BGS approximation and its relationship to our results to DESAI *et al.* (2010), where we calculate the structure of genealogies under our model.

The BGS approximation assumes that deleterious mutations are eliminated by selection quickly compared to the coalescence time between two individuals who do not have any such mutations. When this is true, almost all neutral mutations we observe occurred in individuals that did not have any deleterious mutations, because they have little time to occur in individuals that do have deleterious mutations before these individuals are eliminated by selection. Thus, according to the BGS approximation, the genetic diversity among neutral sites linked to negatively selected sites is exactly the same as the entirely neutral case, but

with the population size N replaced by the size of the least-loaded class. That is, N is replaced by the effective population size

$$N_e = Nh_0 = Ne^{-U_d/s}. \quad (40)$$

Given this N_e , BGS predicts that any properties of neutral diversity are identical to those of coalescent theory with the appropriate N_e . Applying this to the allelic diversity, this predicts that the sampling properties of neutral alleles will be given by the classical Ewens' sampling formula, using $\theta = 2NU_n h_0 = 2NU_n e^{-U_d/|s|}$. Note this is effectively a NM-BGS case, which seems most natural. An alternative NS-BGS case can be defined using $\theta = 2N(U_n + U_d)h_0$; this leads to similar conclusions.

We graph the predictions of the NS interpretation of BGS in Fig. 4 and Fig. 5 (this provides a slightly better prediction than than the NM interpretation). We see that for the case of strong selection, $U_d \ll s$, the NS-BGS approximation predicts slightly higher homozygosity than the NS-ESF (similarly, for $U_d \ll s$ the NM-BGS would be a small shift towards higher homozygosity from the NM-ESF predictions). Keeping in mind that the BGS approach is not meant to describe the diversity at the deleterious sites themselves, this is a reasonable correction to the neutral expectations. However, we see that for weaker selection, $U_d \gtrsim s$, the BGS prediction breaks down dramatically. It predicts that the neutral homozygosity increases dramatically, since the least-loaded class becomes negligible in size. However, the homozygosity is not so large in reality, as our predictions demonstrate. Rather, both neutral and deleterious variation among individuals that harbor one or more deleterious mutations is important. Our theory accounts for this effect, while BGS fails because the approximation that the coalescence time between individuals is dominated by the time in the least-loaded class breaks down.

We explore the comparison to BGS and the reasons for the breakdown of the BGS approximation for $U_d \gtrsim s$ in more detail in DESAI *et al.* (2010). Here, we merely note that, contrary to the intuition one might be tempted to draw from BGS, having more deleterious mutations can never decrease allelic diversity. That is, if we fix all other parameters, simply having more deleterious mutations (i.e. increasing U_d) does not reduce heterozygosity. Certainly it reduces *neutral* heterozygosity, but accounting for all variation a population with a larger deleterious mutation rate will have more allelic heterozygosity.

Failure of an Effective Population Size Description:

The above discussion makes clear that for given population sizes, mutation rates, and selection strengths, purifying selection changes the probabilities of particular allelic configurations in a sample. However, this does not necessarily imply that selection leads to *distortions* in the patterns of genetic variation compared to the neutral case. In the neutral case, the probabilities of all allelic configurations in a sample are determined by a single parameter θ . This means that we can infer θ from a statistic which depends on the probabilities of one set of allelic configurations, and this θ then predicts the expected distribution of all other statistics describing genetic variation within the population, provided it is evolving neutrally.

In this section, we show that there is no effective population size N_e which can describe genetic diversity in our model. That is, the genetic diversity is not equivalent to the diversity in a neutral model for *any* θ . This implies statistical power must exist to distinguish negative selection from neutral processes at a reduced effective population size. This result is in striking contrast to the background selection approximation (BGS).

To see that there is no effective neutral population size N_e to describe diversity in our model, it is sufficient to show that the effective θ that one would infer from one statistic predicts the incorrect values of other statistics. The simplest way to do this is to begin with the Q_2 we would predict given some set of parameters. We calculate the effective θ_e one would infer from this Q_2 using the neutral ESF (i.e. we choose θ_e such that $Q_2 = \frac{1}{1+\theta_e}$). We then calculate the neutral prediction for $Q_{2,1}$ (or Q_3) based on this θ_e . We compare this with our predictions for $Q_{2,1}$ (or Q_3) given the real parameters. The difference between these two predictions is a measure of the deviation from neutrality. We show this deviation from neutrality, expressed as the ratio of the neutral effective population size prediction to the actual result, for $Q_{2,1}$ in Fig. 6a and for Q_3 in Fig. 6b.

We see from Fig. 6 that negative selection distorts the allelic diversity away from high-frequency polymorphisms and towards lower-frequency polymorphisms, for a given level of overall heterozygosity. The effects are strongest when U_d is of order (or slightly larger than) s , and the distortion is stronger for smaller U_n and N .

These two simple statistics measuring deviations from neutrality demonstrate that there is no effective population size describing allelic diversity. This particular comparison is

presumably not the most statistically powerful way to detect this type of negative selection, but it does show that statistical power exists. Using the framework developed in this paper, it is now possible to systematically investigate exactly how linked negatively selected sites generate different patterns of allelic diversity from the neutral case, and to determine which statistics provide the most power detect this type of selection.

While we have shown that there is no neutral effective population size describing allelic diversity, this allelic diversity is a summary statistic of the full per-site diversity. Thus our result also implies that genetic diversity at a per-site level also cannot be described by a neutral effective population size, and that additional power to distinguish neutrality from negative selection can be found in data on site-based variation. We show how our analysis can be used as the basis for calculating this full per-site diversity in a related paper, DESAI *et al.* (2010).

Muller’s Ratchet:

Throughout our analysis, we have assumed that Muller’s ratchet can be neglected. This is clearly not true in general. The problem Muller’s ratchet creates is that h_k can change with time, and this changes the distribution of allele frequencies within each class. After a “click” of the ratchet, the distribution of h_k shifts, eventually reaching a new state shifted left by one class (so the class that was originally at frequency h_k is now at frequency h_{k-1} , and so on). The PRF distribution of lineage frequencies in class k correspondingly shifts from f_k to f_{k-1} , and so on, which changes the allelic diversity.

Fortunately, since $f_k(x)$ is similar to f_{k+1} and f_{k-1} , this effect is unlikely to cause major inaccuracies, provided the ratchet does not click many times over the timescale on which the lineage frequency spectrum turns over. We expect that this is generally true within the bulk of the fitness distribution. At the tails of the distribution, where h_k is small, the allele frequency distribution can sometimes be substantially different than expected due to the ratchet. However, by definition these classes represent a small fraction of the overall population and hence we do not expect them to contribute substantially to allelic diversity.

We tested the accuracy of our approximation neglecting Muller’s ratchet using the simulations described above, all of which included the possibility of the ratchet. Our predictions remain very accurate, even in simulations in which the ratchet was observed to operate. Note, however, that the ratchet is potentially more problematic in considering the genetic

diversity at the level of individual sites, because the high-fitness tail of the fitness distribution can be important for the structure of genealogies even if it does not contribute substantially to allelic diversity at any time. Thus we consider the possible complications introduced by Muller’s ratchet in more detail in DESAI *et al.* (2010).

Conclusion:

We have introduced a formalism to calculate the statistics of allelic diversity in the presence of purifying selection at many linked selected sites. We have done so by calculating the structure of the individual lineages that maintain the deleterious mutation-selection balance.

Our analysis is based on the PRF framework of SAWYER and HARTL (1992), which was originally developed to describe the frequency of mutations at completely unlinked sites. We have adapted this framework to our problem with a shift in perspective: rather than treating new mutations at individual sites as the basic and independently fluctuating quantities, we consider the lineages founded by new mutations as the basic independent quantities. This allows us to describe aspects of the genetic diversity despite the fact that selection is acting on many linked non-independent sites.

Of course, each lineage we describe contains many different mutations, and the fluctuations in lineage frequency described by the PRF framework represent correlated fluctuations in all of these individual mutations. If we could also describe how lineages are related to each other, and hence the statistics of which mutations they share, we could combine this with the results in this paper to describe the full per-site patterns of genetic diversity despite the correlations between sites introduced by linkage and selection. We follow precisely this program in DESAI *et al.* (2010). In this paper, however, we have focused on describing the allelic diversity predicted by our modified PRF framework. This has led to a negatively selected version of the neutral Ewens sampling formula. Most importantly, we found that there is no effective population size that can describe the patterns of allelic diversity in the presence of negative selection at many linked sites.

ACKNOWLEDGEMENTS

We thank Warren Ewens for helpful discussions. AMW thanks the Princeton Center for Theoretical Science at Princeton University, where she was a fellow during the bulk of her

work on this paper. JBP acknowledges support from the James S. McDonnell Foundation, the Alfred P. Sloan Foundation, the David and Lucille Packard Foundation, the Burroughs Wellcome Fund, Defense Advanced Research Projects Agency (HR0011-05-1-0057), and the US National Institute of Allergy and Infectious Diseases (2U54AI057168).

APPENDIX A: INTEGRALS INVOLVING $F_K(X)$

Our expressions for the probabilities of various allelic configurations involve integrals of the form

$$I = \int_0^1 A(x)f(x), \quad (41)$$

where $A(x)$ is a polynomial function of the form $A(x) = x^n(1-x)^m$ (with n and m integers). Here $f(x)$ is the expression from Eq. (9),

$$f(x) = \frac{ah}{e^a - 1} \frac{1}{x(1-x)} [e^{a(1-x)} - 1], \quad (42)$$

where we have suppressed the subscripts and used the notation $a \equiv -2\gamma$.

Whenever n and m are both ≥ 1 , these integrals are easy to evaluate analytically. When either n or m equals zero, the integrals can be separated into an exactly solvable analytical part and a part that involves the integral

$$I' = \int_0^1 \frac{e^{ay} - 1}{y} dy. \quad (43)$$

This integral I' involves the exponential integral special function Ei .

Consider for example the integral

$$I_2 = \int_0^1 x^2 f(x) dx. \quad (44)$$

Substituting in for $f(x)$ and substituting $y = 1 - x$ in the integral gives

$$I_2 = \frac{ah}{e^a - 1} \int_0^1 \frac{1-y}{y} [e^{ay} - 1]. \quad (45)$$

We now simply write $\frac{1-y}{y} = \frac{1}{y} - 1$ and evaluate the analytically solvable parts of this integral to get

$$I_2 = \frac{ah}{e^a - 1} I' - h + \frac{ah}{e^a - 1}. \quad (46)$$

Fortunately, we can calculate a simple analytic approximation for I' in the limit $a \gg 1$ (i.e. $|\gamma| \gg 1$), which is the limit we are always working in. To do this, first consider the integral

$$I'' \equiv \int_{1-\alpha}^1 \frac{e^{ay} - 1}{y} dy = \int_0^\alpha \frac{e^{a(1-x)} - 1}{1-x} dx. \quad (47)$$

We will show that provided $\alpha \gg \frac{1}{a}$ (and note that $\frac{1}{a} \ll 1$ so this includes $\alpha \sim 1$), this integral does not depend on α . Hence we will have $I' = I''$.

We begin by Taylor expanding the factor of $\frac{1}{1-x}$ in the I'' integrand. The number of terms we keep in this Taylor expansion will turn out to be the key to the order in $\frac{1}{a}$ at which our asymptotic form for I' will be valid. The more terms we keep, the higher order in $\frac{1}{a}$ our result will be accurate for. It will turn out that for an integral where $m = 0$ we will need to have an asymptotic expression for I' which is valid up to order $[\frac{1}{a}]^{n-1}$, which means that we will need to use the Taylor expansion of $(1-x)^{-1}$ to $(n-1)^{th}$ order.

For I_2 this means we only need the first order term. So we write

$$I'' \approx [e^{a(1-x)} - 1] [1+x] dx. \quad (48)$$

This can now be evaluated exactly. Doing so, we find

$$I'' = \frac{2}{a}e^a [1 - e^{-a\alpha}] - \alpha - \frac{\alpha^2}{2} - \frac{1}{a}e^a + \frac{1}{a}e^a e^{-a\alpha} - \frac{\alpha}{a}e^a e^{-a\alpha} + \frac{1}{a^2}e^a [1 - e^{-a\alpha}]. \quad (49)$$

Provided $a \gg 1$, we can neglect all terms not involving e^a . Doing this and simplifying, we get

$$I'' = \frac{1}{a}e^a + \frac{1}{a^2}e^a + e^a e^{-a\alpha} \left[-\frac{1}{a^2} - \frac{1}{a} - \frac{\alpha}{a} \right]. \quad (50)$$

Now we can immediately see that provided $\alpha \gg \frac{1}{a}$ (and certainly for $\alpha \sim 1$) this becomes independent of α , and we have simply

$$I'' \approx \frac{1}{a}e^a \left[1 + \frac{1}{a} \right] \approx I'. \quad (51)$$

We can now plug our approximation for I' into our result for I_2 to get

$$I_2 = \frac{h}{a}. \quad (52)$$

For more complex integrals, we need to keep higher order terms in the Taylor expansion of $\frac{1}{1-x}$ used to calculate I' . The general form for this Taylor expansion is $\frac{1}{1-x} = \sum_{m=0}^{\infty} x^m$. Using this form and making the same $a \gg 1$ approximation as above, we find that for arbitrarily complex integrals we can use the form

$$I' = \frac{1}{a}e^a \sum_{m=0}^{\infty} \left[\frac{m!}{a^m} \right]. \quad (53)$$

This in turn means that we have in general

$$I_n = \int_0^1 x^n f(x) = \frac{(n-1)!h}{a^{n-1}}. \quad (54)$$

Similar calculations can be used to find an analogous approximation for $I_m = \int_0^1 (1-x)^m f(x)$, but this integral is not necessary for our purposes in this paper.

These calculations allow us to give simple analytic expressions for any integrals of the form $\int x^n (1-x)^m f(x)$. Whenever m and n are both ≥ 1 , the integrals can be evaluated exactly in terms of elementary functions, and when either m or n are 0 we can use the above results to provide simple analytic approximations to whatever precision we require.

LITERATURE CITED

- BARTON, N. H., 1998 The effect of hitch-hiking on neutral genealogies. *Genetical Research* **72**: 123–133.
- BARTON, N. H. and A. M. ETHERIDGE, 2004 The effect of selection on genealogies. *Genetics* **166**: 1115–1131.
- BETANCOURT, A. J., J. J. WELCH, and B. CHARLESWORTH, 2009 Reduced effectiveness of selection caused by a lack of recombination. *Current Biology* **19**: 655–660.
- BUSTAMANTE, C. D., J. WAKELY, S. SAWYER, and D. L. HARTL, 2001 Directional selection and the site-frequency spectrum. *Genetics* **159**: 1779–1788.
- CHARLESWORTH, B., 1994 The effect of background selection against deleterious mutations on weakly selected, linked variants. *Genetical Research* **63**: 213–227.
- CHARLESWORTH, B., M. T. MORGAN, and D. CHARLESWORTH, 1993 The effect of deleterious mutations on neutral molecular variation. *Genetics* **134**: 1289–1303.
- CHARLESWORTH, D., B. CHARLESWORTH, and M. T. MORGAN, 1995 The pattern of neutral molecular variation under the background selection model. *Genetics* **141**: 1619–1632.
- COMERON, J. A. and M. KREITMAN, 2002 Population, evolutionary and genomic consequences of interference selection. *Genetics* **161**: 389–410.
- COMERON, J. M., A. WILLIFORD, and R. M. KLIMAN, 2008 The Hill-Robertson effect: Evolutionary consequences of weak selection and linkage in finite populations. *Heredity* **100**: 19–31.
- DESAI, M. M., A. WALCZAK, and J. B. PLOTKIN, 2010 The structure of genealogies in the presence of purifying selection: An effective coalescent theory.
- ETHIER, S. N. and T. G. KURTZ, 1987 The infinitely-many alleles model with selection as a measure-valued diffusion. *Stochastic Models in Biology, Lecture Notes in Biomathematics* **70**: 72–86.
- ETHIER, S. N. and T. G. KURTZ, 1994 Convergence to Fleming-Viot processes in the weak atomic topology. *Stochastic Processes and their Applications* **54**: 1–27.
- EWENS, W. J., 1972 The sampling theory of selectively neutral alleles. *Theoretical Population Biology* **3**: 87–112.
- EWENS, W. J., 2004 *Mathematical Population Genetics: I. Theoretical Introduction*. Springer, New York, NY.
- EWENS, W. J. and W.-H. LI, 1980 Frequency spectra of neutral and deleterious alleles in a finite population. *Journal of Mathematical Biology* **10**: 155–166.
- GILLESPIE, J., 2001 Is the population size of a species relevant to its evolution? *Evolution* **55**: 2161–2169.
- GILLESPIE, J. H., 2000 Genetic drift in an infinite population: The pseudohitchhiking model. *Genetics* **155**: 909–919.
- GRIFFITHS, R. C., 1983 Allele frequencies with genic selection. *Journal of Mathematical Biology* **17**: 1–10.
- GROTE, M. N. and T. P. SPEED, 2002 Approximate Ewens formulae for symmetric overdominance selection. *Annals of Applied Probability* **12**: 637–663.
- HAHN, M. W., 2008 Toward a selection theory of molecular evolution. *Evolution* **62**: 255–265.
- HAIGH, J., 1978 The accumulation of deleterious genes in a population-Muller’s ratchet. *Theoretical Population Biology* **14**: 251–267.
- HARTL, D. L. and S. A. SAWYER, 1994 Selection intensity for codon bias. *Genetics* **138**: 227–234.

- HILL, W. and A. ROBERTSON, 1966 The effect of linkage on limits to artificial selection. *Genetical Research* **8**: 269–294.
- JOYCE, P., 1995 Robustness of the Ewens sampling formula. *Journal of Applied Probability* **32**: 609–622.
- JOYCE, P. and S. TAVARE, 1995 The distribution of rare alleles. *Journal of Mathematical Biology* **33**: 602–618.
- LI, W.-H., 1977 Maintenance of genetic variability under mutation and selection pressures in a finite population. *PNAS* **74**: 2509–2513.
- LI, W.-H., 1978 Maintenance of genetic variability under the joint effect of mutation, selection and random drift. *Genetics* **90**: 349–382.
- LI, W.-H., 1979 Maintenance of genetic variability under the pressure of neutral and deleterious mutations in a finite population. *Genetics* **92**: 647–667.
- MCVEAN, G. A. T. and B. CHARLESWORTH, 2000 The effects of Hill-Robertson interference between weakly selected mutations on patterns of molecular evolution and variation. *Genetics* **155**: 929–944.
- SAWYER, S. A. and D. L. HARTL, 1992 Population genetics of polymorphism and divergence. *Genetics* **132**: 1161–1176.
- SEGER, J., W. A. SMITH, J. J. PERRY, J. HUNN, Z. A. KALISZEWSKA, L. L. SALA, L. POZZI, V. J. ROWNTREE, and F. R. ADLER, 2010 Gene genealogies strongly distorted by weakly interfering mutations in constant environments. *Genetics* **184**: 529–545.
- WATTERSON, G. A., 1978 The homozygosity test of neutrality. *Genetics* **88**: 405–417.

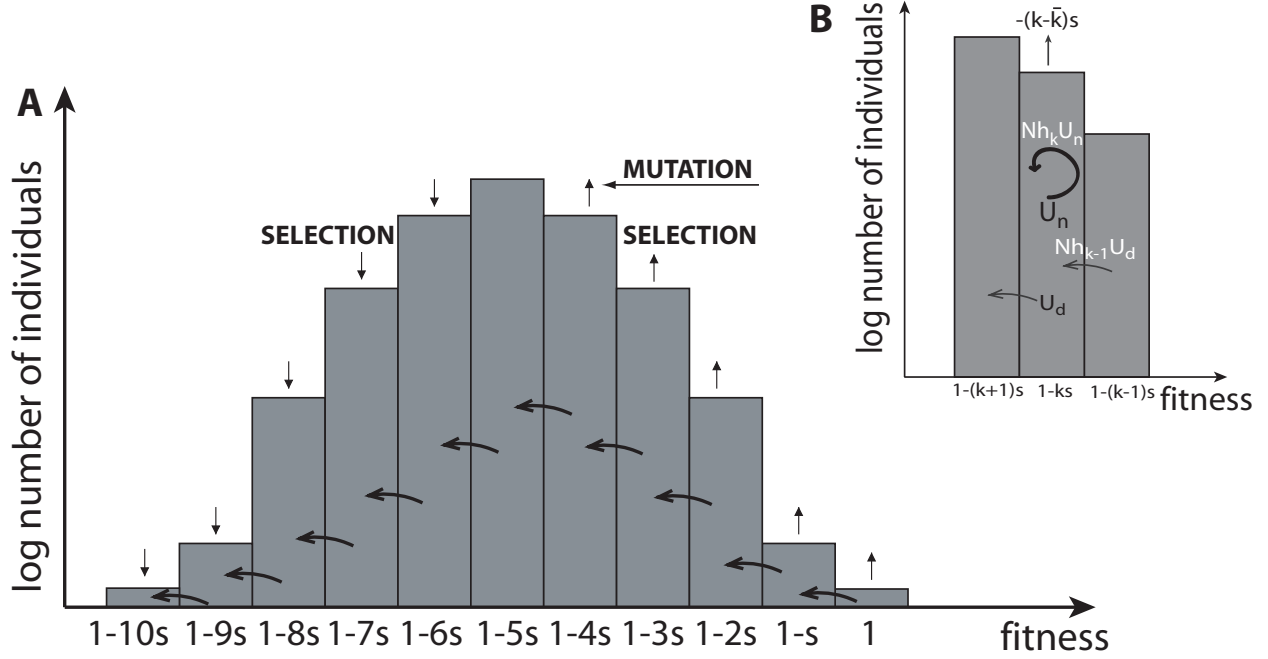


FIG. 1 Schematic of the allelic diversity in the mutation-selection balance. (a) Sketch of the mutation-selection balance in the case $\frac{U_d}{s} = 5$. The steady state distribution of fitness within the population is maintained by a balance between mutations moving individuals towards lower fitness and selection favoring those classes more fit than average at the expense of those less fit than average. (b) The inset shows the processes maintaining a class of individuals with k deleterious mutations. Deleterious mutations from class $k - 1$ found new lineages within class k at rate $Nh_{k-1}U_d$. Neutral mutations found new lineages in the class at a rate Nh_kU_n . Selection favors or disfavors individuals from each lineage at a per capita rate $-(k - \bar{k})s$, and deleterious mutations eliminate individuals from each lineage at a per capita rate $U_d + U_n$.

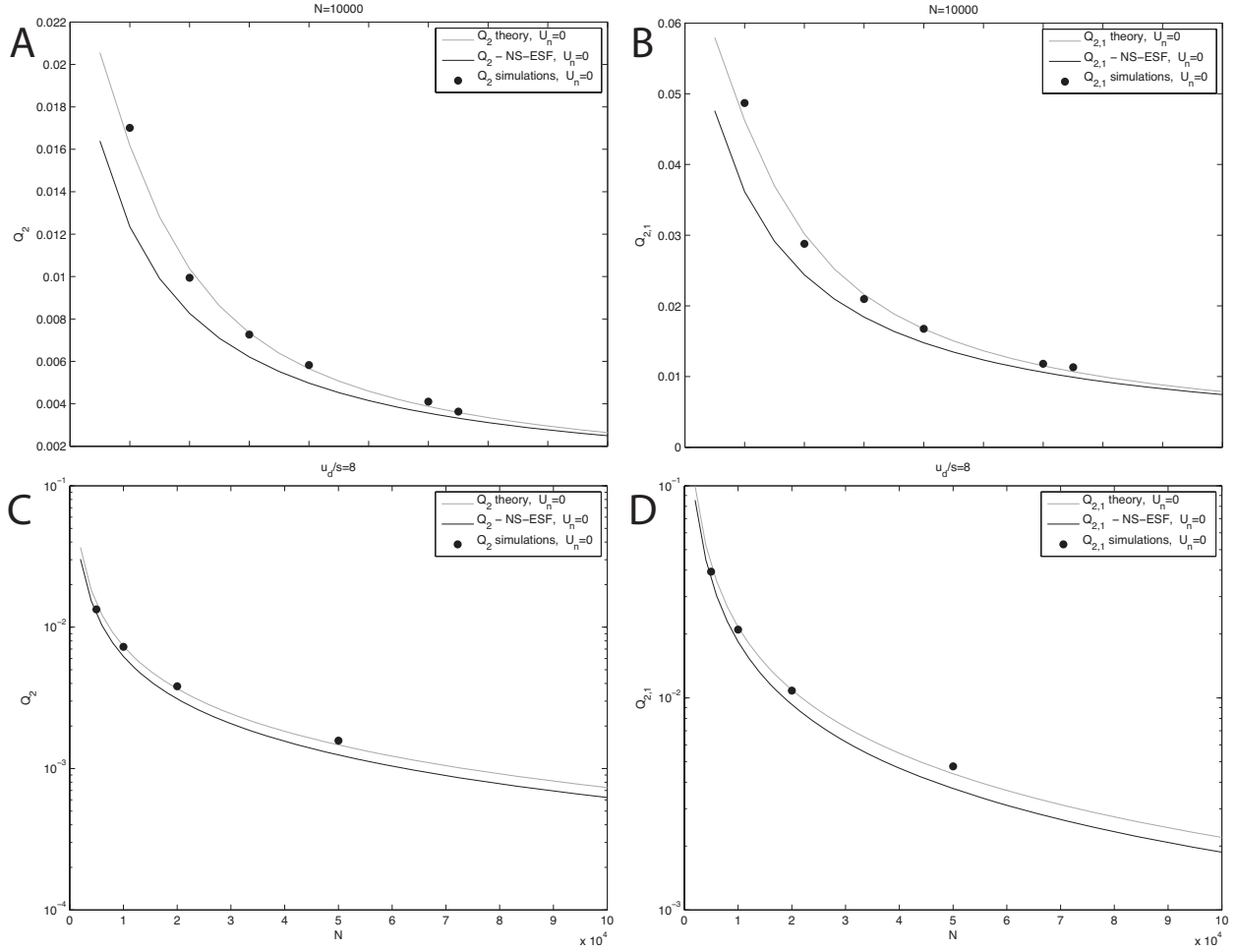


FIG. 2 A comparison between simulation results (dots) and the predictions of our theory (gray lines), for the case where all mutations are deleterious. For comparison we also show the predictions of NS interpretation of the neutral Ewens Sampling formula (black lines; the NM interpretation gives a worse fit to the data). (a) Homozygosity Q_2 as a function of U_d/s for $N = 10^4$. (b) $Q_{2,1}$ as a function of U_d/s for $N = 10^4$. (c) Homozygosity Q_2 as a function of N for $U_d/s = 12$. (d) $Q_{2,1}$ as a function of N for $U_d/s = 12$. In all plots $U_n = 0$, $s = 10^{-3}$.

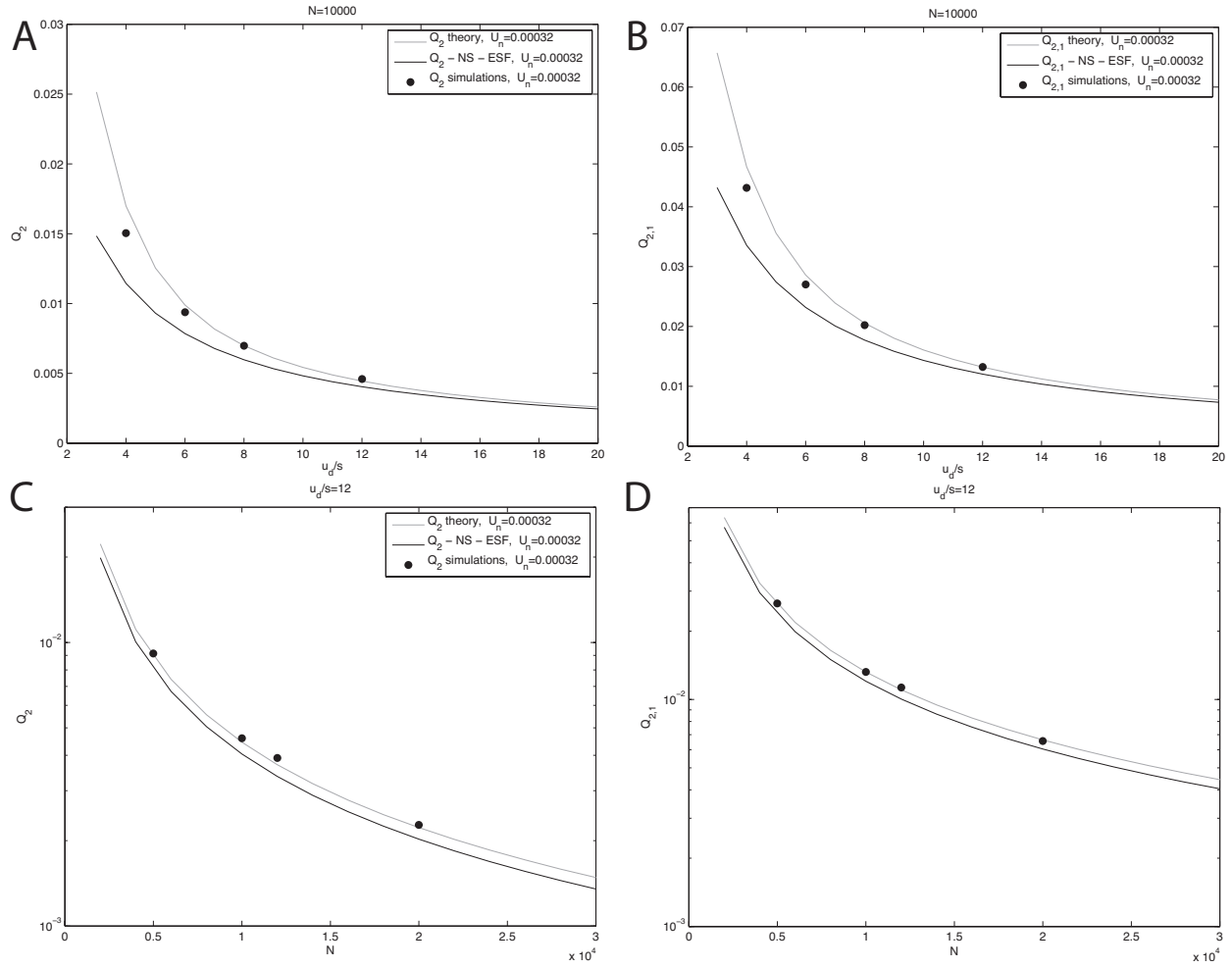


FIG. 3 A comparison between simulation results (dots) and the predictions of our theory (gray lines), for the case where some mutations are deleterious and others are neutral. For comparison we also show the predictions of NS interpretation of the neutral Ewens Sampling formula (black lines; the NM interpretation gives a worse fit to the data). **(a)** Homozygosity Q_2 as a function of U_d/s for $N = 10^4$. **(b)** $Q_{2,1}$ as a function of U_d/s for $N = 10^4$. **(c)** Homozygosity Q_2 as a function of N for $U_d/s = 12$. **(d)** $Q_{2,1}$ as a function of N for $U_d/s = 12$. In all plots $U_n = 3.2 \times 10^{-4}$, $s = 10^{-3}$.

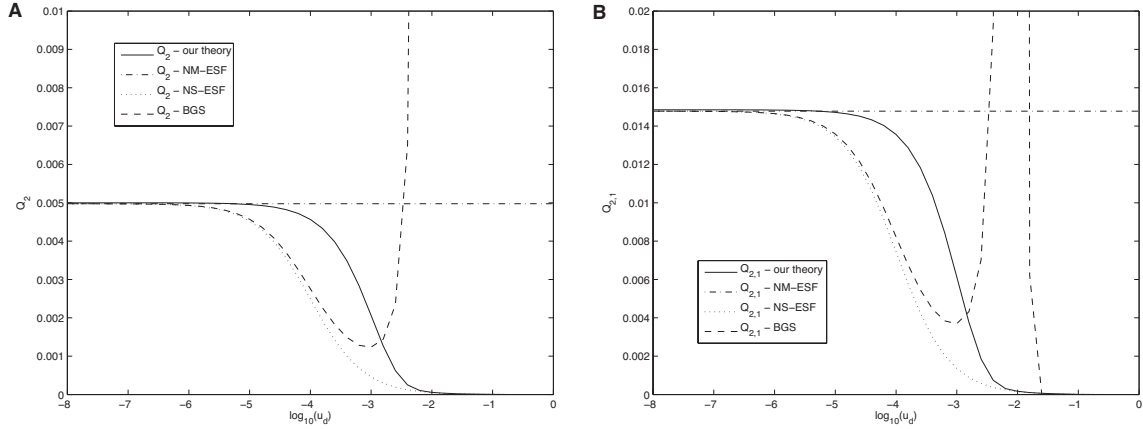


FIG. 4 Allelic diversity as a function of $\ln U_d$, for $U_n = 10^{-4}$, $s = 10^{-3}$, and $N = 10^6$. Our predictions are shown as a solid line, compared to the predictions of the NS-ESF (dotted line) and NM-ESF (dash-dotted line). We also compare our results to the predictions of a neutral ESF using the effective population size that would be predicted by background selection (BGS, dashed line), though we emphasize this is not the situation the BGS approximation was developed to address. **(a)** Homozygosity Q_2 . **(b)** $Q_{2,1}$. Note that $Q_3 \approx 0$ everywhere for these parameters, so for these predictions $Q_{1,1,1} \approx 1 - Q_{2,1}$.

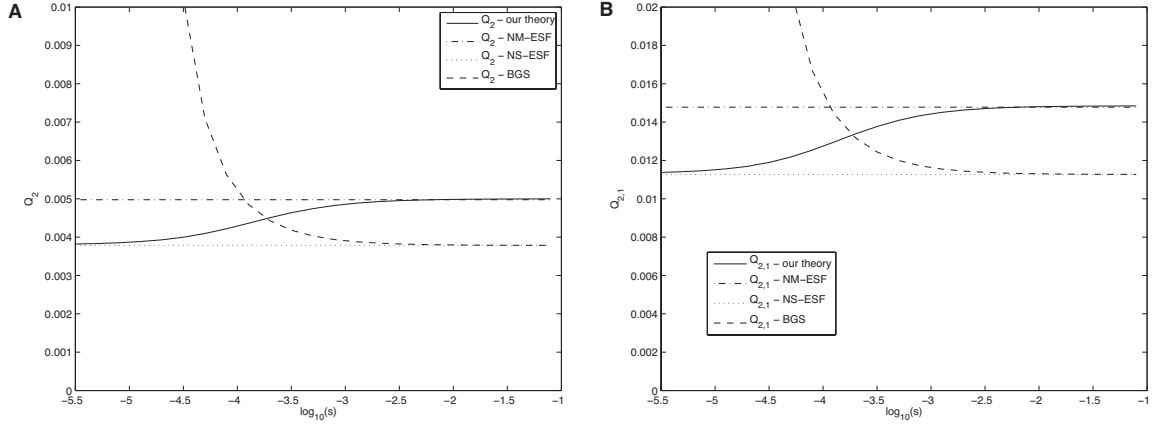


FIG. 5 Allelic diversity as a function of $\ln s$, for $U_n = 10^{-4}$, $N = 10^6$, and $U_d = 10^{-4.5}$. Our predictions are shown as a solid line, compared to the predictions of the NS-ESF (dotted line) and NM-ESF (dash-dotted line). We also compare our results to the predictions of a neutral ESF using the effective population size that would be predicted by background selection (BGS, dashed line), though we note that this is not the situation the BGS approximation was developed to address. (a) Homozygosity Q_2 . (b) $Q_{2,1}$. Note that $Q_3 \approx 0$ everywhere for these parameters, so for these predictions $Q_{1,1,1} \approx 1 - Q_{2,1}$.

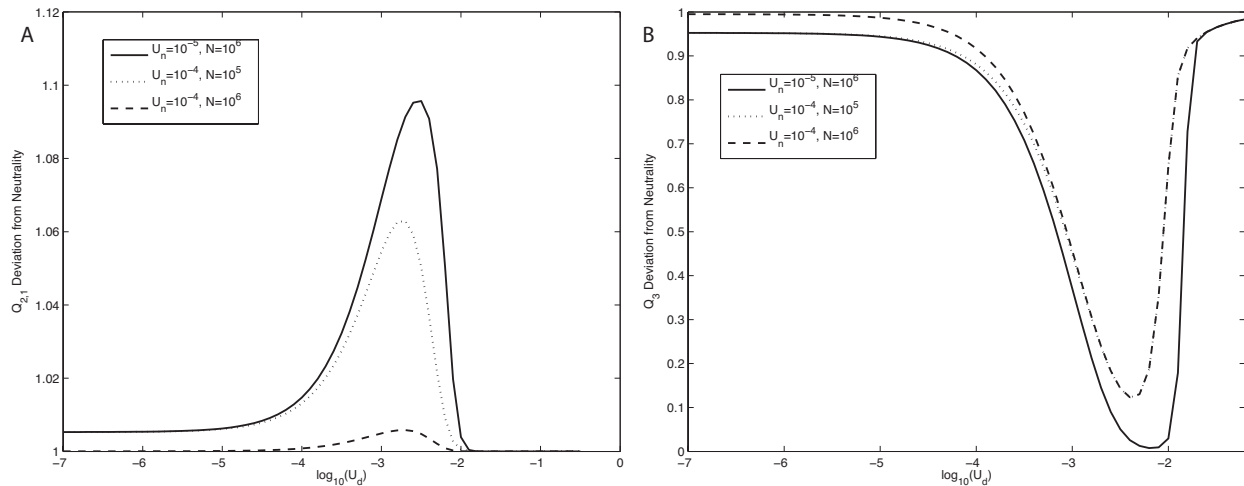


FIG. 6 The deviation from neutrality. We take Q_2 as predicted by our theory, and use the neutral ESF to find the effective θ that this implies by setting $Q_2 = \frac{1}{1+\theta_e}$. We then use this effective θ_e in the neutral ESF to predict the values of $Q_{2,1}$ and Q_3 it corresponds to. We compare this to the $Q_{2,1}$ and Q_3 predicted by our theory. This is a measure of the deviation from neutrality, the skew in the frequency spectrum of allelic diversity away from neutral results with some modified effective population size. **(a)** The ratio of $Q_{2,1}$ from the effective population size description to the $Q_{2,1}$ from our theory, as a function of $\ln(U_d)$, for $s = 10^{-3}$ and three different values of U_n and N . **(b)** The ratio of Q_3 from the effective population size description to the Q_3 from our theory as a function of $\ln(U_d)$, for $s = 10^{-3}$ and three different values of U_n and N .